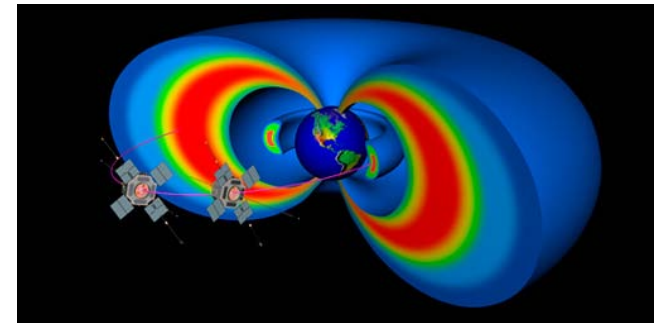


Role of ULF Waves in Transport and Acceleration of Radiation Belt Electrons

Lou Lanzerotti
NJIT



Content

1. Radial diffusion (ULF variations) from start of radiation belt research
 1. Ground-based magnetic and electric (one example) field
 2. Satellite-based particle and magnetic field
2. Non-adiabatic process(es): plasma instabilities (drift mirror example)
 1. Satellite-based particle and magnetic field

Early work: radial diffusion

Magnitude and effectiveness: magnetic; electric; combination

$$\frac{\partial F}{\partial t} = L^2 \frac{\partial}{\partial L} \left(\frac{D_{LL}}{L} \frac{\partial F}{\partial L} \right)$$

$$L^{-10} D_{LL} = 4.8 \cdot 10^3 (f_0/B_0)^2 \beta_H(f_0) \times (9.33 \cdot 10^3 f_0)^{s-2} (L/M)^{(s-2)/2} \mathbf{d}^{-1}$$

Equatorial mirroring; relativistic electrons

Magnetic: Ground data? How related to space data?

Compare ground and space

Very early work: “counting” sudden commencements and sudden impulses.

Ground data: Why bother?

Because hard to obtain continuous magnetic field data in orbit and at all L-shells to evaluate D_{LL} over entire magnetosphere and all local times: what is a given drift shell seeing?

Ground data coverage conceivably very good.

Remains a challenging, fruitful, and important problem for trapped particle studies.

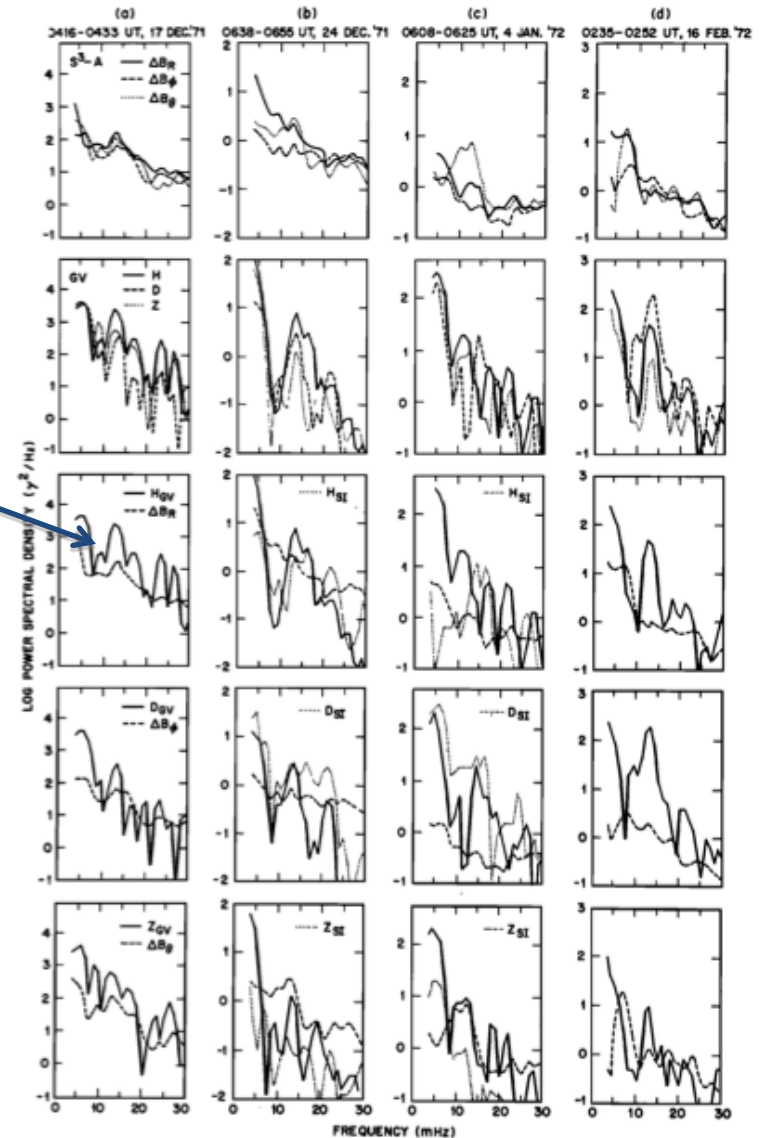
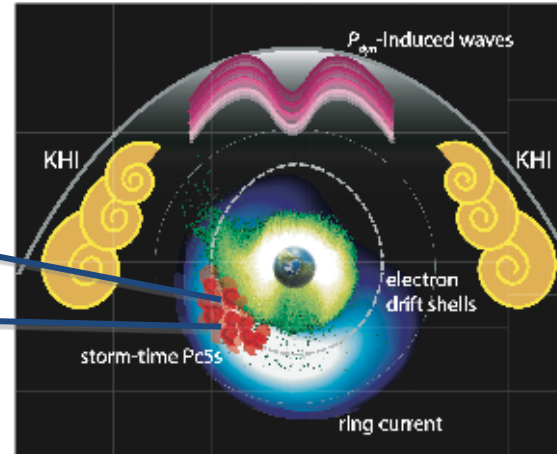
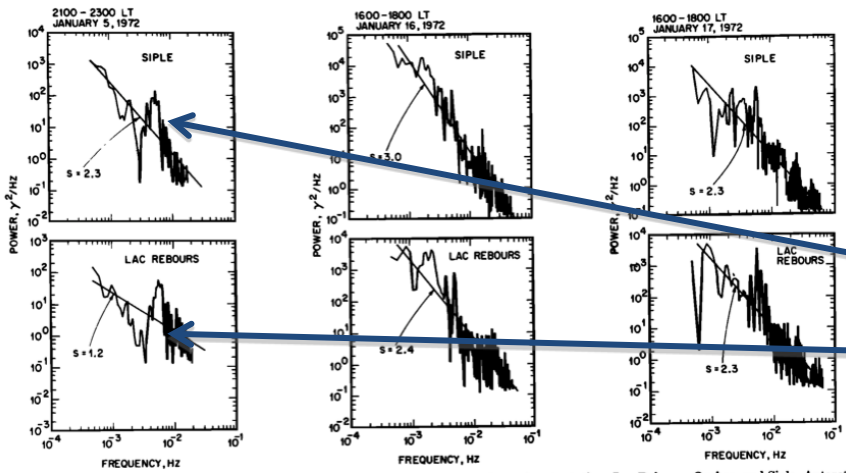


Fig. 5. Power spectra of the data from Explorer 45 (S^A, top panel) and GV (second panel) and comparisons between the Explorer 45 and GV spectra (bottom three panels). Siple spectra are indicated by the dotted lines in the bottom three panels for events B and C. The 90% confidence levels of the Explorer 45 spectra are 0.9 on the log scale.

Power spectra conjugate areas; $L \sim 4$

LM



USTA

Diffusion coefficient $L \sim 4$

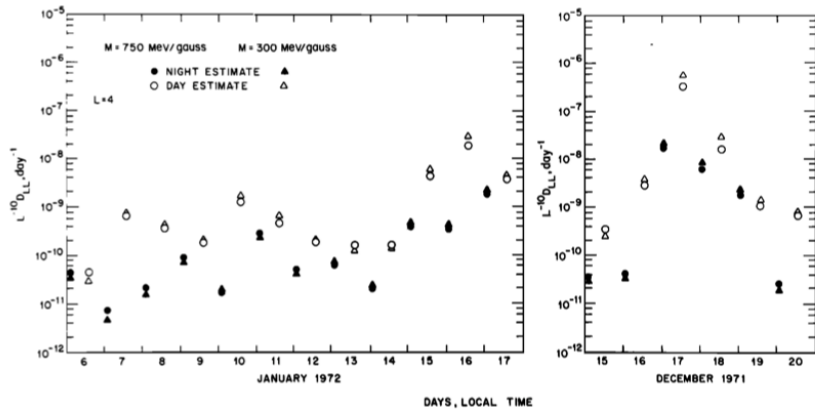


Fig. 6. Plot, as a function of time, of $L^{-10} D_{LL}$ as determined from day and night spectral estimates for electrons with $M = 300$ and 750 Mev/gauss.

Geosynchronous orbit magnetic field analysis: ATS-5 spacecraft

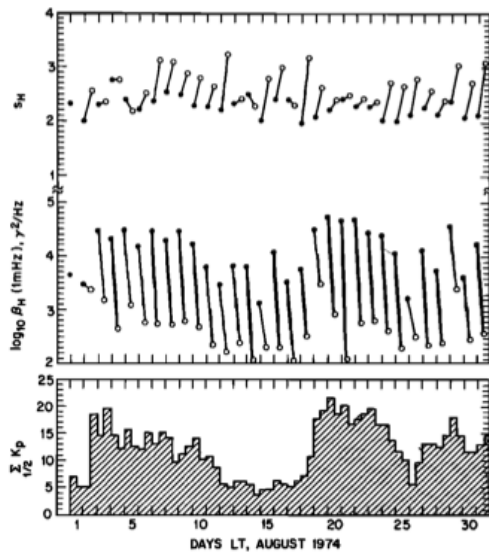


Fig. 1. Local time dependence of weighted spectral power at 1 mHz and spectral slope for local day (open circles) and local night (solid circles) averages for August 1974. At the bottom are plotted the $\frac{1}{2}$ -day sum of the magnetic activity index. A dependence of magnetic power on K_p is clearly seen.

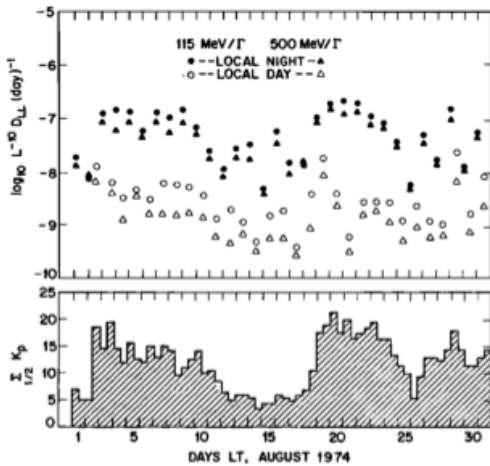


Fig. 2. Local time dependence of the radial diffusion coefficient determined from local day spectral averages (open symbols), local night spectral averages (solid symbols), and for particles of two different first invariants. At the bottom are plotted the $\frac{1}{2}$ -day sum of the magnetic activity index.

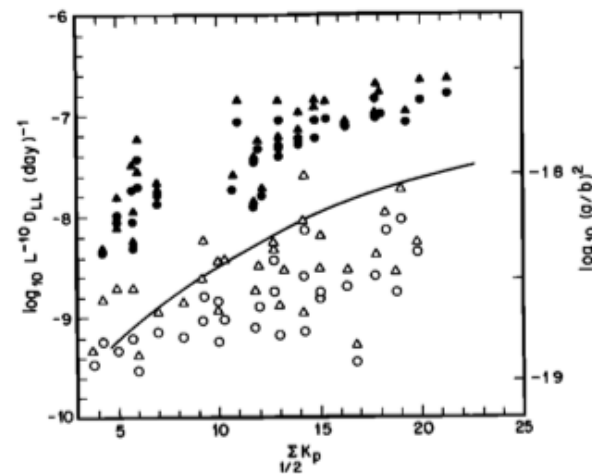


Fig. 4. Radial diffusion coefficient as a function of the $\frac{1}{2}$ -day sum of the geomagnetic activity index K_p . The solid line plots the statistical dependence of the stagnation point of the magnetosphere on the geomagnetic activity index, assuming the daily sum of K_p is just twice a $\frac{1}{2}$ -day sum.

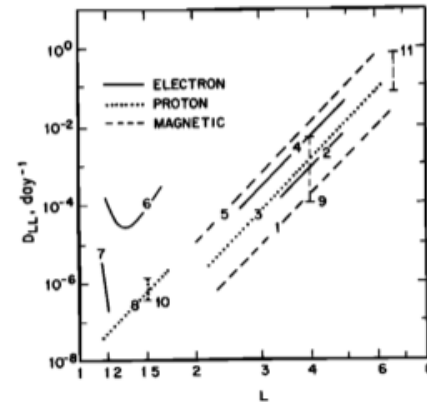
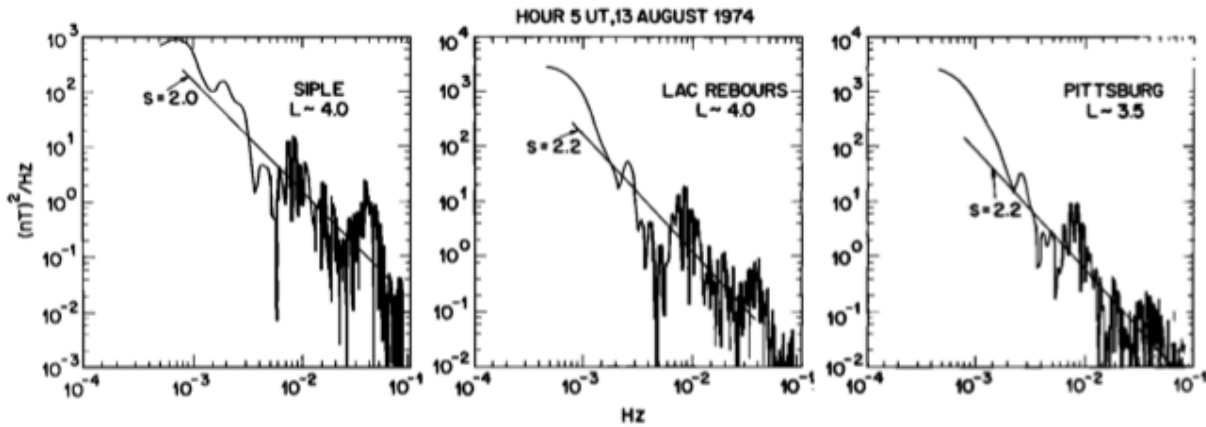


Fig. 5. Summary plot of radial diffusion coefficients from previously published analyses: 1, Nakada and Mead [1965]; 2, Lanzerotti et al. [1970]; 3, Söraas [1969] and Nakada and Mead [1965]; 4, Newkirk and Walt [1968a]; 5, Toerskoy [1965]; 6, Farley [1969]; 7, Newkirk and Walt [1968b]; 8, Farley and Walt [1971]; 9, Lanzerotti and Morgan [1973]; 10, Claffin and White [1974]; and 11, present analysis.



LW

Fig. 1. Power spectra of the H component geomagnetic field fluctuations measured at three ground-based magnetic stations during hour 5 UT, August 13, 1974. The slope of a least squares power law fit to each spectrum is indicated.

Comparisons of D_{LL} values from various sources, including particle, magnetic, electric

LW

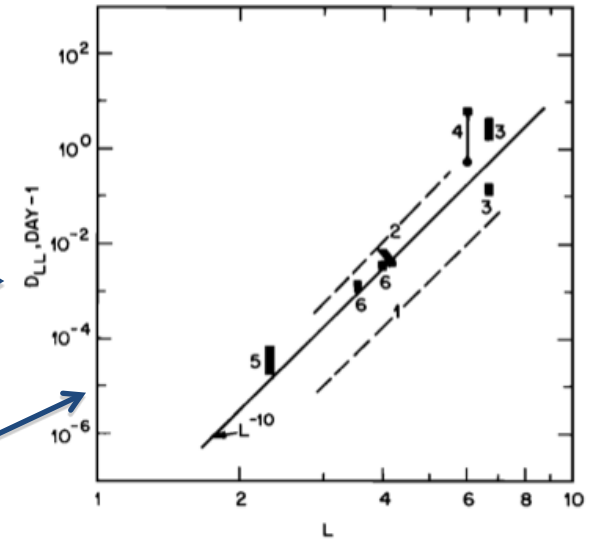
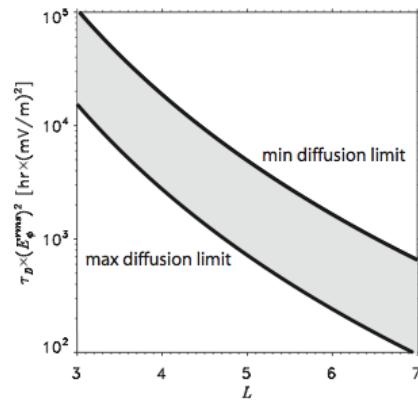


Fig. 2. Comparison of selected estimates of particle radial diffusion coefficients made from measures of electric and magnetic field fluctuations. Where possible, values of the published estimates are given for particles with comparable first adiabatic invariants. (1) Estimate of Nakada and Mead [1965] from magnetic sudden commencements; (2) Estimate of Tverskoy [1965] from magnetic sudden impulses and commencements; (3) Estimates of Lanzerotti *et al.* [1978] from in-situ magnetic field fluctuations for particles with $M = 300, 750$ MeV/G. The lower and upper estimates are derived separately from fluctuating field measurements made during local day and local night, respectively; (4) Estimates of Holzworth and Mozer [1979] from electric field fluctuations. The upper and lower points correspond to particles with $M \sim 800$ and ~ 80 MeV/G, respectively; (5) Estimate of Andrews [1979] from electric field fluctuations. The estimate is for $M \sim 40$ MeV/G; (6) Present results from Table 1 for $M = 300, 750$ MeV/G.



USTA

Fig. 4. Characteristic timescales of radial transport due to stormtime Pc5s normalized to the root-mean-square amplitude of the wave electric field.

Comparisons of radial diffusion coefficient determinations

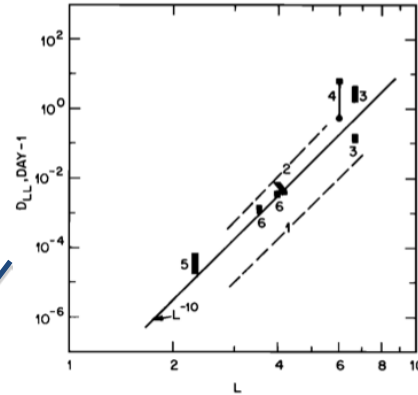


Fig. 2. Comparison of selected estimates of particle radial diffusion coefficients made from measures of electric and magnetic field fluctuations. Where possible, values of the published estimates are given for particles with comparable first adiabatic invariants. (1) Estimate of *Nakada and Mead* [1965] from magnetic sudden commencements; (2) Estimate of *Tversky* [1965] from magnetic sudden impulses and commencements; (3) Estimates of *Lancerotti et al.* [1978] from in-situ magnetic field fluctuations for particles with $M = 300, 750$ MeV/G. The lower and upper estimates are derived separately from fluctuating field measurements made during local day and local night, respectively; (4) Estimates of *Holworth and Mazer* [1979] from electric field fluctuations. The upper and lower points correspond to particles with $M \sim 800$ and ~ 80 MeV/G, respectively; (5) Estimate of *Andrews* [1979] from electric field fluctuations. The estimate is for $M \sim 40$ MeV/G; (6) Present results from Table 1 for $M = 300, 750$ MeV/G.

?

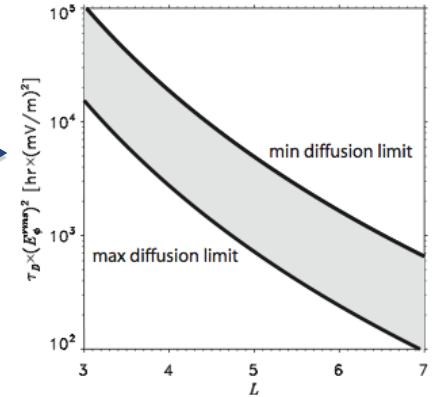


Fig. 4. Characteristic timescales of radial transport due to stormtime Pc5s normalized to the root-mean-square amplitude of the wave electric field.

Smaller?

LW

USTA

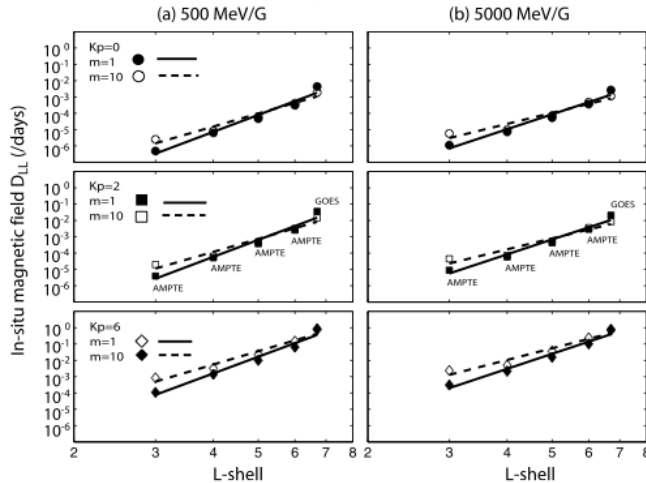


Figure 9. Magnetic field diffusion coefficients derived from in situ magnetic field PSDs measured by AMPTE at $L = 3, 4, 5,$ and 6 as well as GOES at $L = 6.6$. The shaded and un-shaded symbols represent diffusion coefficients derived assuming $m = 1$ and $m = 10$, respectively. The solid and dashed lines represent power law fits to these diffusion coefficients for M -values of (a) 500 MeV/G and (b) 5000 MeV/G.

OMMRMECS

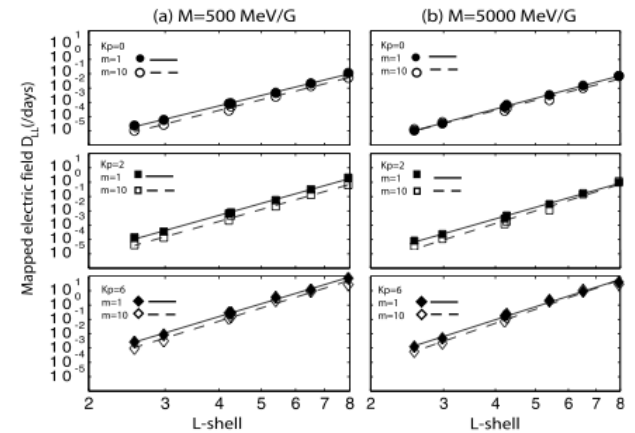


Figure 10. Electric field diffusion coefficients derived from ground magnetic field PSDs mapped to electric field PSDs in space in the equatorial plane with m -values of 1 and 10 . The solid and dashed lines represent power law fits to these diffusion coefficients for M -values of (a) 500 MeV/G and (b) 5000 MeV/G.

Non-adiabatic processes. Can be many. Including various plasma instabilities.
Possible drift mirror instability:

5566

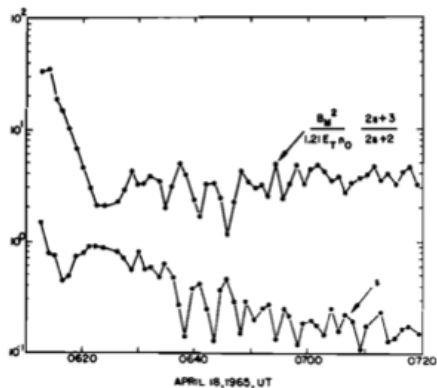
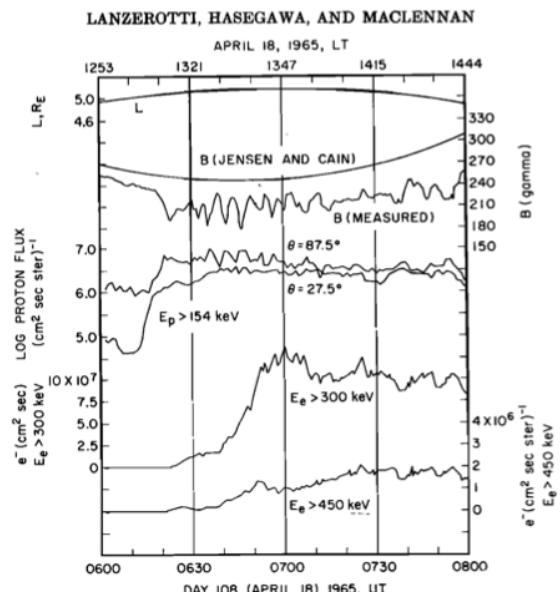


Fig. 7. Plot of the instability criterion and the pitch-angle asymmetry parameter, s , as a function of time.

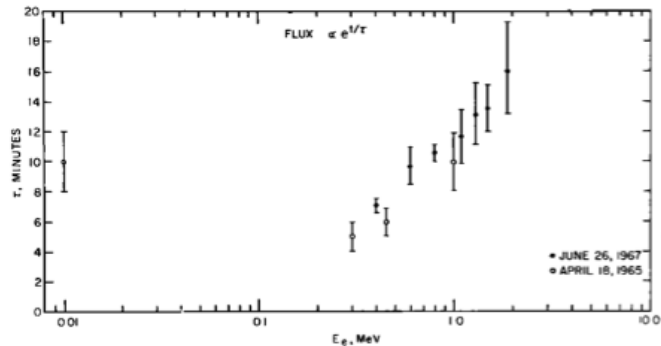
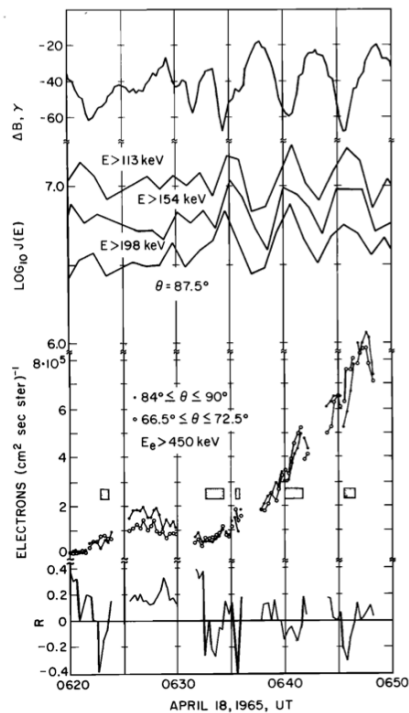


Fig. 10. Plot of the rate of electron heating during the initial large heating observed on both Explorer 26 and ATS 1. Note the data point at 10 keV.

References for sources

LFMC: Observations of Magnetohydrodynamic Waves on the Ground and on a Satellite, L. J. Lanzerotti, H. Fukunishil, C. G. MacLennan, and L. J. Cahill, Jr., *JGR*, **81**, 4537, 1976.

LHM: Drift Mirror Instability in the Magnetosphere: Particle and Field Oscillations and Electron Heating, L. J. Lanzerotti, A. Hasegawa, and C. G. MacLennan, *JGR*, **74**, 5565, 1969.

LM: ULF Geomagnetic Power Near L = 4. 2. Temporal variation of the Radial Diffusion Coefficient for Relativistic Electrons. L. J. Lanzerotti and C. G. Morgan, *JGR*, **78**, 4600, 1973.

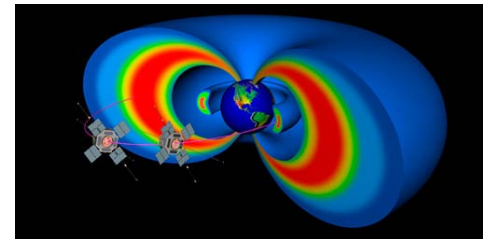
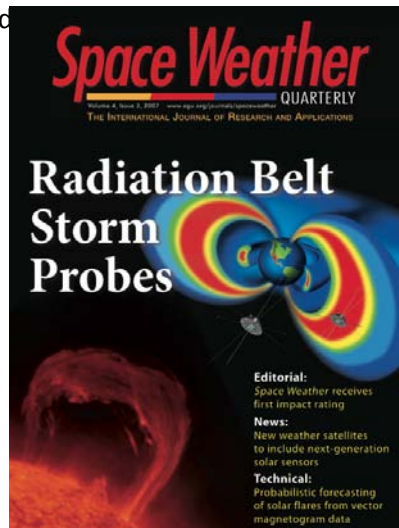
LW: Particle Diffusion in the Geomagnetosphere: Comparison of Estimates from Measurements of magnetic and Electric Field Fluctuation, *JGR*, **85**, 2346, 1980.

LWA: Geomagnetic Field Fluctuations at Synchronous Orbit 2. Radial Diffusion, L. J. Lanzerotti, D. C. Webb, and C. W. Arthur, *JGR*, **83**, 3866, 1978.

OMMRMECS: ULF Wave Derived Radiation Belt Diffusion Coefficients, L. G. Ozeke, I. R. Mann, K. R. Murphy, I. J. Rae, D. K. Milling, S. R. Elkington, A. A. Chan, and H. J. Singer, *JGR*, **A04222**, 2012.

USTA: Radial Transport of radiation Belt Electrons, *Ann. Geophys.*, **27**, 2173, 2009.

Ukhorskiy, M. I. Sitnov, K. Takahashi, and B. J. Anderson,



Thank you!